The Astrophysical Journal, 664:435–442, 2007 July 20

X-RAY, UV, AND OPTICAL OBSERVATIONS OF SUPERNOVA 2006bp WITH *SWIFT*: DETECTION OF EARLY X-RAY EMISSION

S. Immler,[1,2] P. J. Brown,[3] P. Milne,[4] L. Dessart,[4] P. A. Mazzali,[5,6] W. Landsman,[1] N. Gehrels,[7] R. Petre,[1] D. N. Burrows,[3] J. A. Nousek,[3] R. A. Chevalier,[8] C. L. Williams,[1] M. Koss,[1] C. J. Stockdale,[9] M. T. Kelley,[9] K. W. Weiler,[10] S. T. Holland,[1,2] E. Pian,[5] P. W. A. Roming,[3] D. Pooley,[11,12] K. Nomoto,[13] J. Greiner,[14] S. Campana,[15] and A. M. Soderberg[16]

Received 2006 November 15; accepted 2007 March 27

ABSTRACT

We present results on the X-ray and optical/UV emission from the Type II-P supernova (SN) 2006bp and the interaction of the SN shock with its environment, obtained with the X-Ray Telescope (XRT) and UV/Optical Telescope (UVOT) on board *Swift*. SN 2006bp is detected in X-rays at a 4.5 σ level of significance in the merged XRT data from days 1 to 12 after the explosion. If the 0.2–10 keV band X-ray luminosity of $L_{0.2-10} = (1.8 \pm 0.4) \times 10^{39}$ ergs s^{-1} is caused by interaction of the SN shock with circumstellar material (CSM) deposited by a stellar wind from the progenitor's companion star, a mass-loss rate of $\dot{M} \approx (1 \times 10^{-5}\ M_\odot\ \mathrm{yr}^{-1})(v_w/10\ \mathrm{km\ s}^{-1})$ is inferred. The mass-loss rate is consistent with the nondetection in the radio with the VLA on days 2, 9, and 11 after the explosion and is characteristic of a red supergiant progenitor with a mass of $\approx$12–15 $M_\odot$ prior to the explosion. The *Swift* data further show a fading of the X-ray emission starting around day 12 after the explosion. In combination with a follow-up *XMM-Newton* observation obtained on day 21 after the explosion, an X-ray rate of decline of $L_X \propto t^{-n}$ with index $n = 1.2 \pm 0.6$ is inferred. Since no other SN has been detected in X-rays prior to the optical peak, and since Type II-P SNe have an extended "plateau" phase in the optical, we discuss the scenario that the X-rays might be due to inverse Compton scattering of photospheric optical photons off relativistic electrons produced in circumstellar shocks. However, due to the high required value of the Lorentz factor ($\approx$10–100), which is inconsistent with the ejecta velocity inferred from optical line widths, we conclude that inverse Compton scattering is an unlikely explanation for the observed X-ray emission.

Subject headings: circumstellar matter — supernovae: individual (SN 2006bp) — ultraviolet: ISM — X-rays: general — X-rays: individual (SN 2006bp) — X-rays: ISM

Online material: color figures

1. INTRODUCTION

SN 2006bp was discovered on 2006 April 9.6, with an apparent magnitude of 16.7 in unfiltered 20 s CCD exposures using a 0.60 m f/5.7 reflector (Nakano 2006). Subsequent observations by K. Itagaki showed that the SN brightened rapidly between April 9.6 and 9.8 UT. The nondetection in unfiltered ROTSE-IIIb observations on April 9.15 UT (>16.9 mag; Quimby et al. 2006) gives a likely explosion date of 2006 April 9. On the basis of the optical/UV colors (Immler et al. 2006a) observed with *Swift* and the detection of hydrogen and helium lines in ground-based optical spectra (Quimby et al. 2006), SN 2006bp was classified as a core-collapse Type II SN.

The optical/UV light curve established by *Swift* (this work) shows that SN 2006bp belongs to the class of Type II-P SNe, which are characterized by a prolonged "plateau" period of sustained optical flux (see § 3.1). This plateau phase results from recombination in the massive hydrogen envelopes ($\gtrsim 2\ M_\odot$ H mass) of the progenitors. Most massive stars ($\approx$8–25 $M_\odot$) become Type II SNe, approximately 2/3 of which are Type II-P (Heger et al. 2003), depending on the mass and metallicity. Due to the large masses of the progenitor stars and the high abundance of Type II-P SNe, they play a primary role in the formation of neutron stars. Such massive progenitor stars have strong stellar winds that can deposit significant amounts of material in their environments. As the outgoing SN shock runs through the circumstellar matter (CSM) deposited by the stellar wind, large amounts of X-ray emission and radio synchrotron emission can be produced. Four of the 26 SNe detected in X-rays to date[17] are of Type II-P: SN 1999em, SN 1999gi, SN 2002hh, and SN 2004dj

[1] Astrophysics Science Division, X-Ray Astrophysical Laboratory, NASA Goddard Space Flight Center, Greenbelt, MD 20771; stefan.m.immler@nasa.gov.
[2] Universities Space Research Association, 10211 Wincopin Circle, Columbia, MD 21044.
[3] Department of Astronomy and Astrophysics, Pennsylvania State University, University Park, PA 16802.
[4] Steward Observatory, 933 North Cherry Avenue, Tucson, AZ 85721.
[5] INAF, Osservatorio Astronomico di Trieste, via G.B. Tiepolo 11, 34131 Trieste, Italy.
[6] Max-Planck-Institut für Astrophysik, Karl-Schwarzschild-Strasse 1, 85741 Garching, Germany.
[7] Astrophysics Science Division, Astroparticle Physics Laboratory, NASA Goddard Space Flight Center, Greenbelt, MD 20771.
[8] Department of Astronomy, University of Virginia, Charlottesville, VA 22904.
[9] Department of Physics, Marquette University, Milwaukee, WI 53201-1881.
[10] Naval Research Laboratory, Washington, DC 20375-5320.
[11] Astronomy Department, University of California at Berkeley, Berkeley, CA 94720.
[12] Chandra Fellow.
[13] Department of Astronomy, School of Science, University of Tokyo, Bunkyo-ku, Tokyo 113-0033, Japan.
[14] Max-Planck-Institut für extraterrestrische Physik, Giessenbachstrasse, 85748 Garching, Germany.
[15] INAF, Osservatorio Astronomico di Brera, via E. Bianchi 46, I-23807 Merate, Italy.
[16] Division of Physics, Mathematics, and Astronomy, California Institute of Technology, Pasadena, CA 91125.
[17] See http://lheawww.gsfc.nasa.gov/users/immler/supernovae_list.html for a complete list of X-ray SNe and references.

TABLE 1
Swift Observations of SN2006bp

Sequence (1)	Date (UT) (2)	XRT Exp. (s) (3)	UVOT Exp. (s) (4)
30390001	2006 Apr 10 12:47:26	4333	4917
30390003	2006 Apr 11 03:22:00	4323	4301
30390004	2006 Apr 12 08:19:01	3157	2770
30390005	2006 Apr 12 03:30:00	1705	1684
30390006	2006 Apr 13 03:37:00	6906	6660
30390007	2006 Apr 14 08:38:01	748	746
30390008	2006 Apr 14 16:39:01	868	899
30390009	2006 Apr 14 08:34:01	156	155
30390010	2006 Apr 14 16:36:01	4	4
30390011	2006 Apr 15 07:06:01	3373	3296
30390012	2006 Apr 15 18:22:01	1572	1544
30390013	2006 Apr 16 05:36:00	260	260
30390014	2006 Apr 16 18:29:00	80	81
30390015	2006 Apr 16 05:39:01	3013	2995
30390016	2006 Apr 16 18:30:02	1537	1526
30390017	2006 Apr 17 04:04:01	3666	3494
30390018	2006 Apr 17 18:35:01	1639	1612
30390019	2006 Apr 18 07:23:00	61	57
30390020	2006 Apr 18 07:27:01	2609	2935
30390021	2006 Apr 20 14:00:01	3174	3118
30390022	2006 Apr 21 06:04:01	363	364
30390023	2006 Apr 21 06:09:01	2741	2743
30390024	2006 Apr 22 02:57:00	2801	2749
30390025	2006 Apr 23 03:03:01	742	743
30390026	2006 Apr 23 03:07:01	5248	5221
30390027	2006 Apr 24 01:32:01	2999	2733
30390028	2006 Apr 26 01:43:00	1782	1642
30390029	2006 Apr 28 00:50:01	2829	2693
30390030	2006 May 1 10:14:01	974	965
30390031	2006 May 1 11:50:01	3793	3914
30390032	2006 May 4 04:06:01	2542	2450
30390034	2006 May 10 00:21:40	884	873
30390036	2006 May 22 12:17:00	622	863
30390037	2006 May 22 12:34:01	633	976
30390038	2006 May 30 08:32:01	5242	5143

Note.—Col. (1): *Swift* sequence number; col. (2): date, in units of Universal Time (UT); col. (3): X-Ray Telescope (XRT) exposure time, in units of seconds; col. (4): Ultraviolet/Optical Telescope (UVOT) exposure time, in units of seconds.

(see Tables 1 and 2 and references in Chevalier et al. 2006). Mass-loss rate estimates from the X-ray and radio observations are between a few times 10^{-6} to 10^{-5} $M_{\odot}$ yr^{-1}(v_w/10 km s^{-1}), where v_w is the pre-SN stellar wind velocity.

In this paper we present the earliest observation and detection of a SN in X-rays to date, starting 1 day after the explosion. In addition to the *Swift* X-ray observations and a follow-up *XMM-Newton* X-ray observation, we discuss the broadband spectral energy distribution during the early evolution (days to weeks) of SN 2006bp, as well as multiepoch UV spectra obtained with *Swift*.

2. OBSERVATIONS

2.1. *Swift UVOT Optical/UV Observations*

The Ultraviolet/Optical Telescope (UVOT; Roming et al. 2005) and X-Ray Telescope (XRT; Burrows et al. 2005) on board the *Swift* observatory (Gehrels et al. 2004) began observing SN 2006bp on April 10.54 UT. The HEASOFT[18] (version 6.1.1) and *Swift* Software (version 2.5, build 19) tools and latest calibration products were used to analyze the data.

The SN was detected with the UVOT at R.A. $= 11^{\rm h}53^{\rm m}55.70^{\rm s}$, decl. $= +52^{\circ}21'10.4''$ (equinox J2000.0), with peak magnitudes of $V = 15.1$, $B = 15.4$, $U = 14.5$, UVW1 [216–286 nm FWHM] = 14.7, UVM2 [192–242 nm] = 15.1, and UVW2 [170–226 nm] = 14.8. Statistical and systematic errors are 0.1 mag each.

On the basis of the UVOT photometry and the $V - B$ and $B - U$ colors, the SN was classified as a young Type II event (Immler et al. 2006a). The classification was confirmed by Hobby-Eberly Telescope (HET) spectra taken on day 2, showing a blue continuum and a narrow absorption line at 592 nm, consistent with Na I in the rest frame of the host galaxy, NGC 3953 (z = 0.00351; Verheijen & Sancisi 2001); a narrow emission line consistent with rest-frame Hα; a broad absorption line around 627 nm; and a narrow but slightly broadened emission line at 583 nm (Quimby et al. 2006).

Thirty-five individual exposures were obtained between April 10.54 UT and May 30.45 UT (see Table 1 for an observation log). Assuming an explosion date of April 9, the observations correspond to days 1–51 after the explosion.

Swift optical, UV, and X-ray images of SN 2006bp and its host galaxy NGC 3953 (Hubble type SBbc; NED) are shown in Figure 1. The UVOT six-filter light curve of SN 2006bp is given in Figure 2.

2.2. *Swift Grism Observations*

The UVOT includes two grisms for obtaining spectra in the UV and visible bands. The UV grism has a nominal wavelength range of 1800–2900 Å, while the V grism has a wavelength range of 2800–5200 Å. The UV grism also records spectra in the 2900–4900 Å range, but at half the sensitivity of the V grism, and with the possibility of contamination by second-order overlap. We obtained six UV grism spectra and one V grism spectrum of SN 2006bp. The four earlier grism observations had moderate to severe contamination from the host galaxy and bright stars in the field and are not used in this study. The successful grism

[18] Available at http://heasarc.gsfc.nasa.gov/docs/software/lheasoft.

TABLE 2
UVOT Grism Observations of SN2006bp

Days after Explosion (1)	Sequence (2)	Mode (3)	$T_{\rm start}$ (UT) (4)	Exposure (s) (5)	$N_{\rm exp}$ (6)
9	00030390020	UV	2006 Apr 18 07:30:28	2431	2
12	00030390023	V	2006 Apr 21 06:10:22	2688	2
14	00030390026	UV	2006 Apr 23 03:10:13	3252	4

Note.—Col. (1): Days after the explosion of SN 2006bp (2006 April 9); col. (2): *Swift* sequence number; col. (3): UVOT grism mode; col. (4): exposure start time in units of UT; col. (5): exposure time in units of seconds; col. (6): number of individual exposures.

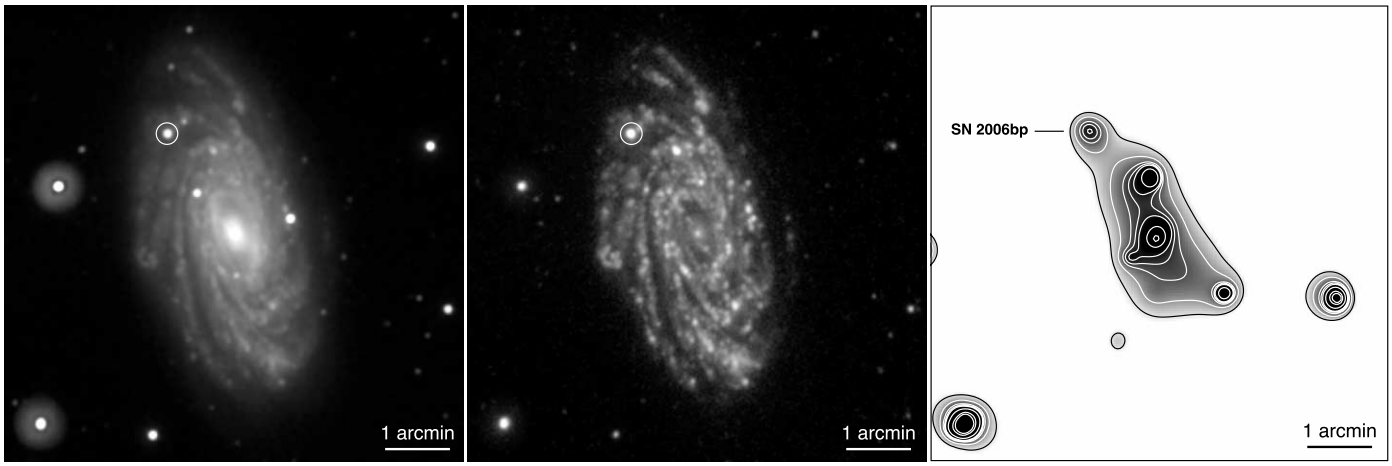

FIG. 1.—*Swift* optical, UV, and X-ray images of SN 2006bp and its host galaxy, NGC 3953. *Left*: *Swift* optical image, constructed from the UVOT *V* (750 s exposure time; *red*), *B* (1966 s; *green*), and *U* (1123 s; *blue*) filters obtained from 34 co-added images taken between 2006 April 10.54 UT and 2006 May 30.45 UT. The optical images are slightly smoothed with a Gaussian filter of 1.5 pixels (FWHM). The position of SN 2006bp is indicated by a white circle of 10″ radius. The size of the image is 6.5′ × 6.5′. *Middle*: UV image, constructed from the co-added UVOT UVW1 (750 s exposure time; *red*), UVM2 (1966 s; *green*), and UVW2 (1123 s; *blue*) filters obtained between 2006 April 10.54 UT and 2006 May 30.45 UT. The UV images are slightly smoothed with a Gaussian filter of 1.5 pixels (FWHM). Same scale as at left. *Right*: X-ray image at 0.2–10 keV, constructed from the merged 41.4 ks XRT data and adaptively smoothed to achieve a signal-to-noise ratio in the range 2.5–4. Contour levels are at 0.3, 0.6, 0.9, 1.5, 3, 6, 12, and 20 counts pixel^{-1}. Same scale as the optical and UV images. [*See the electronic edition of the Journal for a color version of this figure*.]

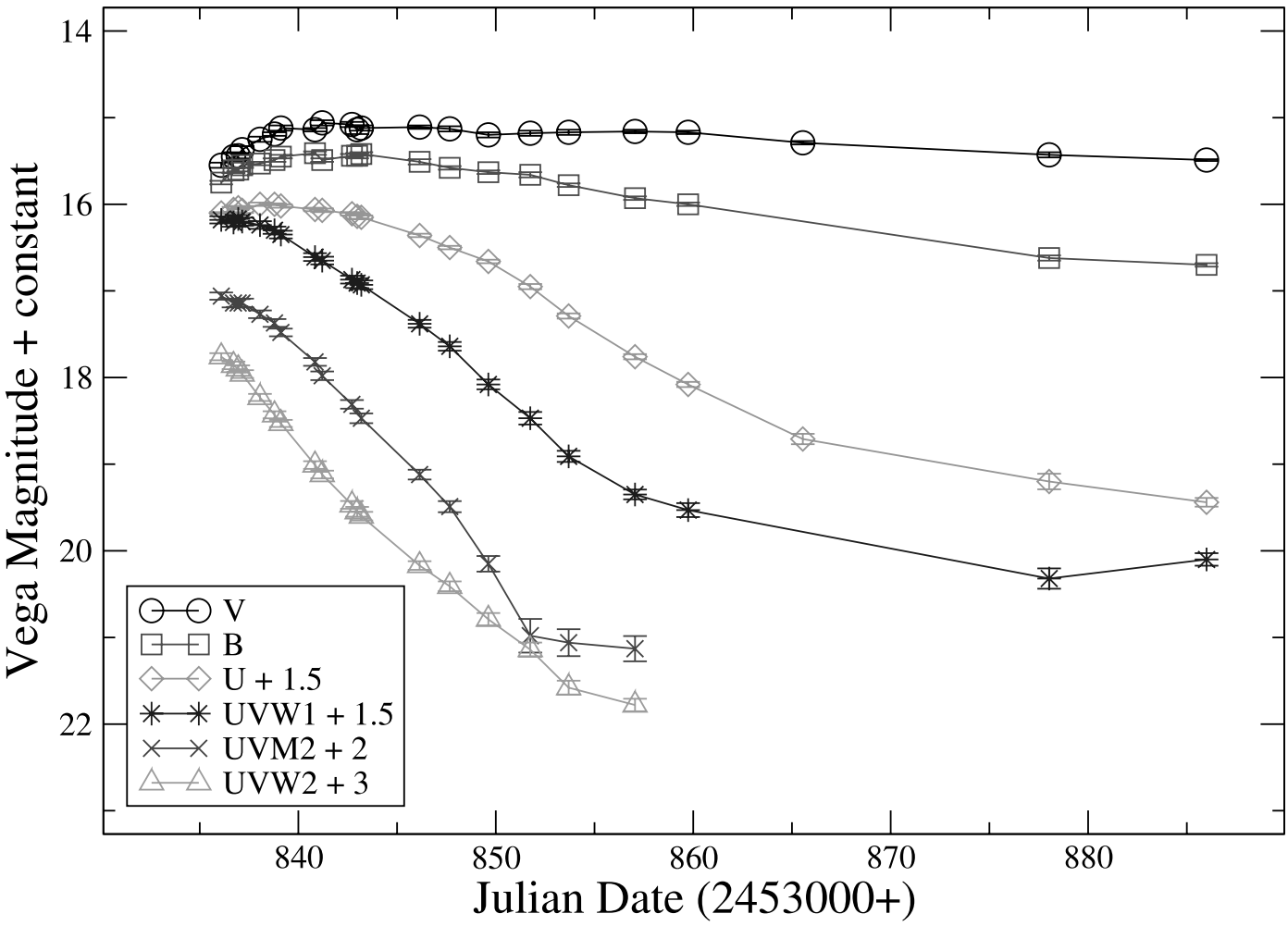

FIG. 2.—*Swift* UVOT light curve of SN 2006bp obtained in all six filters. The *U*, UVW1, UVM2, and UVW2 light curves were shifted down vertically by 1.5, 1.5, 2, and 3 mag, respectively, to avoid overlap. [*See the electronic edition of the Journal for a color version of this figure*.]

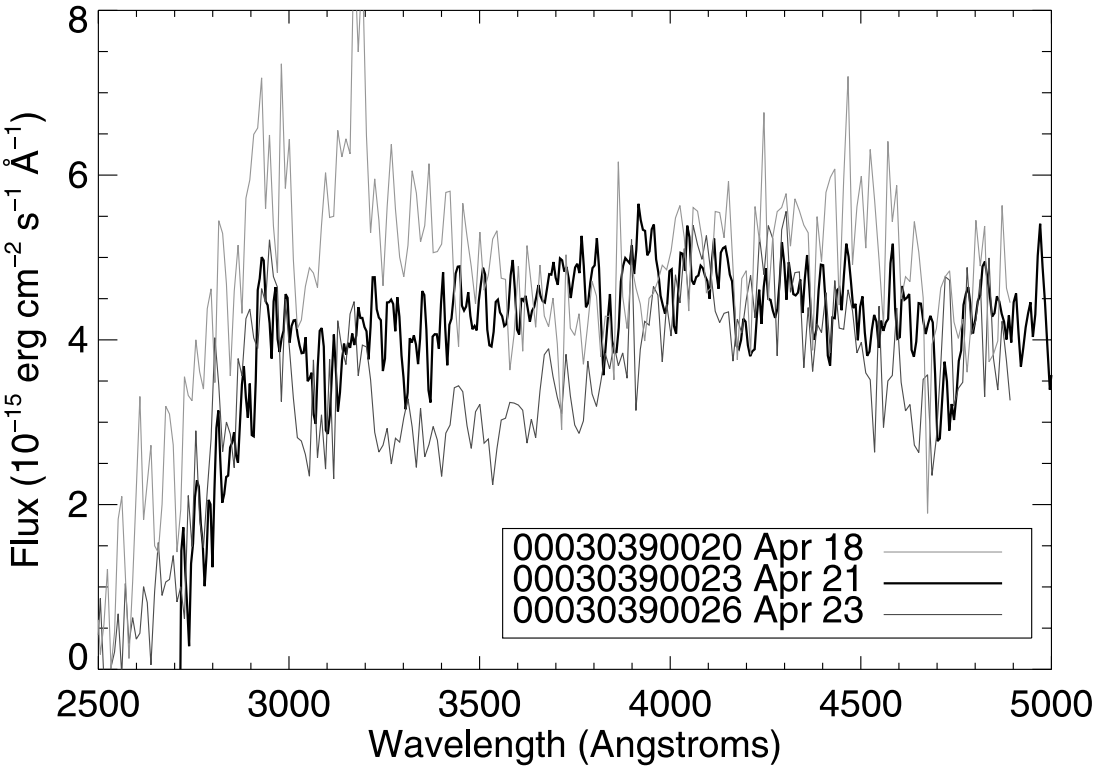

FIG. 3.—*Swift* UV grism observations of SN 2006bp obtained on 2006 April 18, 21, and 23, corresponding to days 9, 12, and 14 after the explosion. [*See the electronic edition of the Journal for a color version of this figure.*]

observations are shown in Figure 3. A log of the observations is given in Table 2.

2.3. *Swift XRT Observations*

The *Swift* XRT observations were obtained simultaneously with the UVOT and grism observations. X-ray counts were extracted from a circular region with an aperture of 10 pixel (24″) radius centered at the position of the SN. The background was extracted locally from a source-free region of radius of 1′ to account for detector and sky background and for a low level of residual diffuse emission from the host galaxy.

2.4. *XMM-Newton Observation*

An *XMM-Newton* European Photon Imaging Camera (EPIC) Director's Discretionary Time (DDT) observation was performed on April 30.39 UT (PI S. Immler; Obs-ID 0311791401), corresponding to day 21 after the explosion. SAS[19] (version 7.0.0), FTOOLS[20] (version 6.1.1), and the latest *XMM-Newton* calibration products were used to analyze the *XMM-Newton* data. Inspection of the EPIC pn and MOS data for periods with a high particle background showed no contamination of the data, which resulted in clean exposure times of 21.2 ks for the pn and 22.9 ks for each of the two MOS instruments.

2.5. *VLA Radio Observation*

Radio observations were performed with the VLA[21] at three epochs (days 2, 9, and 11) with a search for radio emission conducted within a radius of 10″ of the optical position (Nakano 2006) using AIPS.[22] Upper limits (3 σ) to any radio flux density were established at <0.414 mJy on 2006 April 11.97 UT (spectral luminosity $<1.1 \times 10^{26}$ ergs s^{-1} Hz^{-1} for an assumed distance of 14.9 Mpc) at 22.46 GHz (wavelength 1.3 cm) and <0.281 mJy at 8.460 GHz (wavelength 3.5 cm), on 2006 April 18.27 at <0.498 mJy at 14.94 GHz (wavelength 2.0 cm), and on 2006 April 20.16 at <0.276 mJy at 22.46 GHz and <0.143 mJy at 8.460 GHz (Kelley et al. 2006). Although only uncertain mass-loss rate estimates can be obtained from radio nondetections, under standard assumptions ($v_w = 10$ km s^{-1}, $v_s = 10^4$ km s^{-1}, $T_{\rm CSM} = 3$–10×10^4 K, and $m = 1.0$; see, e.g., Weiler et al. 2002; Lundqvist & Fransson 1988), the upper limit to the radio-determined pre-SN mass-loss rate is estimated to be 10^{-6}–10^{-5} $M_\odot$ yr^{-1}.

3. RESULTS

3.1. *Swift UVOT Optical/UV Observations*

The *Swift V*-band UVOT observations show that the SN reached its maximum brightness around day 7 after the estimated time of explosion, faded slightly over the next few days, and subsequently reached a plateau phase characteristic for Type II-P SNe (see Fig. 2). At increasingly shorter wavelengths, the SN shows an earlier maximum and steeper rates of decline. In the roughly linear period 5–15 days after the explosion, the decay slopes are approximately 0.21, 0.25, 0.16, 0.06, 0.02, and 0.01 mag day^{-1} in the UVW2, UVM2, UVW1, *U*, *B*, and *V* bands, respectively.

3.2. *Swift and XMM-Newton X-Ray Observations*

An X-ray source is detected in the merged 41.4 ks *Swift* XRT observations obtained between days 1 and 12 after the explosion

[19] Available at http://xmm.vilspa.esa.es/sas.

[20] Available at http://heasarc.gsfc.nasa.gov/docs/software.html.

[21] The VLA telescope of the National Radio Astronomy Observatory is operated by Associated Universities, Inc., under a cooperative agreement with the National Science Foundation.

[22] Available at http://www.aoc.nrao.edu/aips.

TABLE 3
X-RAY OBSERVATIONS OF SN2006bp

Days after Explosion (1)	Instrument (2)	Exposure (ks) (3)	S/N (σ) (4)	Count Rate (10^{-3}) (5)	f_X (10^{-14}) (6)	L_X (10^{39}) (7)
1–5	*Swift* XRT	20.0	4.4	1.31 ± 0.30	6.94 ± 1.58	1.84 ± 0.42
6–12	*Swift* XRT	21.5	4.4	1.25 ± 0.29	6.58 ± 1.52	1.75 ± 0.40
13–31	*Swift* XRT	23.1	<3	<0.81	<4.00	<1.06
21	*XMM-Newton* EPIC pn	21.2	4.9	3.0 ± 0.6	1.4 ± 0.3	0.38 ± 0.08

NOTE.—Col. (1): Days after the explosion of SN 2006bp (2006 April 9); col. (2): instrument used; col. (3): exposure time, in units of ks; col. (4): significance of source detection, in units of Gaussian sigma; col. (5): 0.2–10 keV count rate, in units of 10^{-3} counts s^{-1}; col. (6): 0.2–10 keV X-ray band unabsorbed flux, in units of 10^{-14} ergs cm^{-2} s^{-1}; col. (7): 0.2–10 keV X-ray band luminosity, in units of 10^{39} ergs s^{-1}.

at R.A. = $11^h53^m56.1^s$, decl. = $+52°21'11.1''$ (positional error $3.5''$), consistent with the optical position of the SN. The aperture-, background-, and vignetting-corrected net count rate is $(1.3 \pm 0.3) \times 10^{-3}$ counts s^{-1} (0.2–10 keV band). Two additional X-ray sources are detected within the D_{25} diameter of the host galaxy, as well as an X-ray source associated with the nucleus of the host galaxy (see Fig. 1). The chance probability of any of the three X-ray sources being within a radius of $3.5''$ at the position of SN 2006bp is estimated to be 1.5×10^{-3}.

Adopting a thermal plasma spectrum with a temperature of $kT = 10$ keV (see Fransson et al. 1996 and references therein) and assuming a Galactic foreground column density with no intrinsic absorption ($N_H = 1.58 \times 10^{20}$ cm^{-2}; Dickey & Lockman 1990) gives a 0.2–10 keV X-ray band unabsorbed flux and luminosity of $f_{0.2-10} = (6.8 \pm 1.6) \times 10^{-14}$ ergs cm^{-2} s^{-1} and $L_{0.2-10} = (1.8 \pm 0.4) \times 10^{39}$ ergs s^{-1}, respectively, for a distance of 14.9 Mpc ($z = 0.00351$, per Verheijen & Sancisi [2001], with $H_0 = 71$ km s^{-1} Mpc^{-1}, $\Omega_\Lambda = 2/3$, and $\Omega_m = 1/3$).

The SN is not detected in the merged 23.1 ks XRT data obtained between days 12 and 31 after the explosion. The (3σ) upper limit to the X-ray count rate is $<8.1 \times 10^{-4}$ counts s^{-1} (0.2–10 keV), corresponding to an unabsorbed flux and luminosity of $f_{0.2-10} < 4 \times 10^{-14}$ ergs cm^{-2} s^{-1} and $L_{0.2-10} < 1 \times 10^{39}$ ergs s^{-1}.

In order to probe the evolution of the X-ray emission in more detail, we subdivided the data taken before day 12 into two observations with similar exposure times of ≈20 ks each (see Table 3). Within the errors of the photon statistics, no significant decline is observed over the first 12 days after the explosion (see Fig. 4).

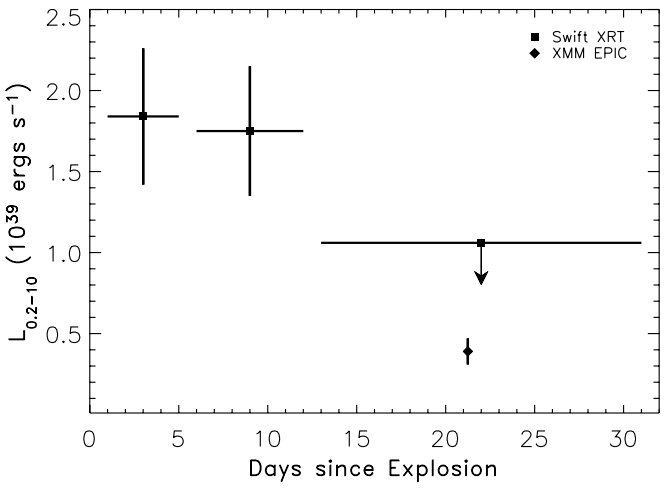

FIG. 4.—X-ray light curve (0.2–10 keV) of SN 2006bp as observed with the *Swift* XRT and *XMM-Newton* EPIC instruments. The time is given in units of days after the outburst (2006 April 9). Vertical error bars indicate statistical 1 σ errors; horizontal error bars indicate the periods covered by the observations (which are not contiguous). The *Swift* XRT upper limit from days 13 to 31 is at a 3 σ level of confidence.

To follow the X-ray rate of decline over a longer period, an *XMM-Newton* observation was obtained on day 21 after the explosion. The SN is detected at a 4.9 σ level of confidence, with an EPIC pn net count rate of $(3.0 \pm 0.6) \times 10^{-3}$ counts s^{-1} (0.2–10 keV band), corresponding to an unabsorbed flux and luminosity of $f_{0.2-10} = (1.4 \pm 0.3) \times 10^{-14}$ ergs cm^{-2} s^{-1} and $L_{0.2-10} = (3.8 \pm 0.8) \times 10^{38}$ ergs s^{-1}.

A best-fit X-ray rate of decline of $L_X \propto t^{-n}$ with index $n = 1.2 \pm 0.6$ is obtained from the *Swift* XRT and *XMM-Newton* detections. The X-ray light curve of SN 2006bp is given in Figure 4. Due to the limited photon statistics of the *Swift* XRT and *XMM-Newton* EPIC data, no detailed spectral fitting is possible.

4. DISCUSSION

4.1. *Ultraviolet Emission*

UV emission from SN explosions can arise from different physical processes. The first photon signature from a core-collapse SN event is thought to be associated with shock breakout, which should manifest itself in a burst of light peaking in the X-rays and the far UV (Ensman & Burrows 1992; Blinnikov & Bartunov 1993; Blinnikov et al. 1998, 2000; Li 2007). The exact duration of this emission can be from hours to days, depending on the progenitor structure. Fast expansion of the ejecta and efficient radiative cooling at its "photosphere" make this epoch short-lived and therefore difficult to observe. At such early times, the object is not bright in the optical and is thus usually still undetected. A SN is usually discovered when it becomes bright in the optical, but by this time the photosphere has cooled too much for X-ray emission. Observational evidence for a shock breakout was provided by *Swift* observations of the gamma-ray burst (GRB) related to SN 2006aj (Campana et al. 2006), although this was probably mediated by a cocoon of material lost by the star before it collapsed.

UV emission has also been observed at early times ($\lesssim$2 weeks) in the photospheric phase of SN ejecta, emanating from the progenitor envelope layers that transition over time from thick to thin when the ejecta are still very hot (e.g., Mazzali 2000). The UV emission is typically strongest during early times (as in the spectrum of SN 1987A on day 1; Pun et al. 1995) and fades substantially over the course of a few days (weak UV emission was detected in an *HST* observation of SN 1993J that occurred 18 days after the explosion; Jeffery et al. 1994; Baron et al. 1994). At later times, after weeks, months, or years, UV emission is in general associated with the interaction of the ejecta with the CSM (Fransson et al. 1987, 2002; Pun et al. 2002). The UV is therefore a very sensitive spectral probe of the fast-changing

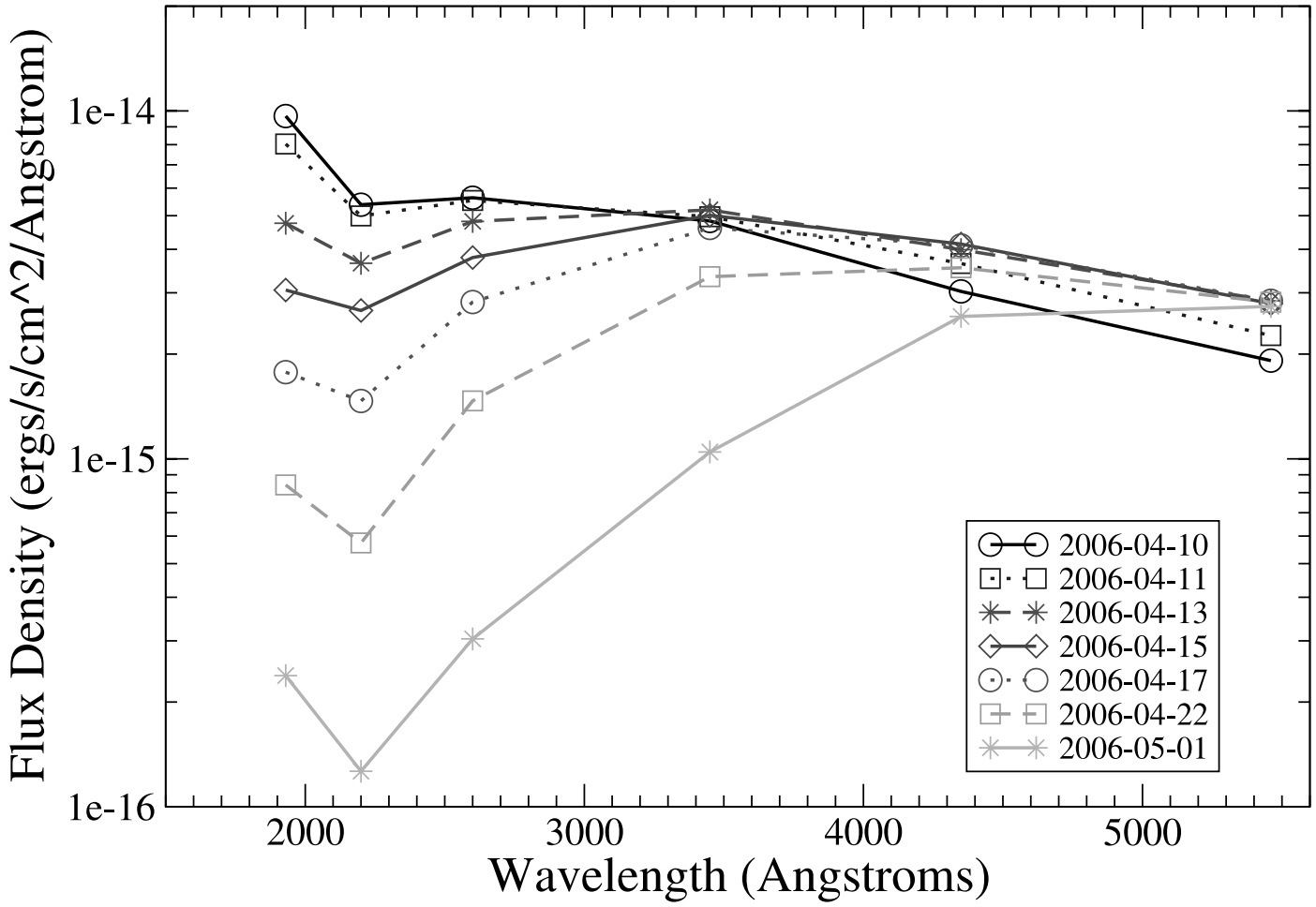

FIG. 5.—Evolution of the spectral energy distribution (SED) of SN 2006bp in the optical/UV wavelength band. The SED was produced from near-simultaneous UVOT observations in all six filters obtained between days 1 and 26 after the explosion (*from top to bottom*). [*See the electronic edition of the Journal for a color version of this figure*.]

conditions in the SN expanding photosphere during the earliest phases.

The first observation of SN 2006bp shows a spectral energy distribution (SED) peak in the UV, rather than in the optical (Fig. 5), which supports the conclusion that the SN was detected very early. Thirty-five observations finely sample the light curve over the 51 days after its discovery, revealing a flux variation in the UV by 2 orders of magnitude. The redward shift of the SED stems from the cooling of the photosphere. There is a direct effect in the reduction of the equivalent blackbody (or effective/electron) temperature (e.g., Mazzali & Chugai 1995), but the main effect is caused by the shift of the opacity from species of higher to lower ionization, as discussed in Eastman & Kirshner (1989) and Dessart & Hillier (2005, 2006).

The main physical process affecting the UV flux distribution is line blanketing (e.g., Lentz et al. 2000; Mazzali 2000). Metal lines, especially lines of Fe II and Fe III, are very numerous in the UV, and the velocity dispersion in the ejecta causes these lines to act as a blanket that blocks the UV flux. Photons absorbed in the UV are reemitted at visible wavelengths, where they can more easily escape (e.g., Mazzali & Lucy 1993; Mazzali 2000). Thus, the UV flux is determined by the ionization state of the SN envelope, as well as by its metal content. Since on average UV Fe III lines are redder than Fe II lines, the sudden transition from Fe III to Fe II when hydrogen recombines in the ejecta of a Type II SN shifts the region where line blanketing is most effective and affects the UV spectrum dramatically (see Figs. 1, 3, and 5 in Dessart & Hillier 2005). This onset of line blanketing is evident in the UV spectra of SN 2006bp as observed by *Swift* (see Fig. 3). The corresponding forest of overlapping lines gives an apparently continuous source of light blocking: at early times, Fe III blanketing operates most strongly between 1500 and 2000 Å, while at later times, Fe II blanketing affects the entire UV range. Combined with this dominant background opacity are a few strong resonance lines of less abundant metals, e.g., Mg II λ2800, which are only visible while metal line blanketing is moderate.

The SED evolution supports the current understanding of the photospheric phase of Type II SNe; however, UV coverage will provide a more extended spectroscopic and photometric analysis. In particular, the unsaturated metal line blanketing together with the fast-changing UV SED provides additional constraints on the temperature evolution, the ejecta ionization and composition, and, importantly, on reddening, that optical observations alone do not guarantee. This will be the subject of a forthcoming study (L. Dessart 2007, in preparation).

4.2. *X-Ray Emission*

X-ray emission from young (days to weeks old) SNe can be produced by the radioactive decay products of the ejecta and by inverse Compton scattering of photospheric photons off relativistic electrons produced during the explosion, as well as

by the interaction of the SN shock with the ambient CSM (forward shock) and SN ejecta (reverse shock).

While several of the emission lines characteristic of the radioactive decay products have been observed in SN 1987A (e.g., McCray 1993), the total X-ray output is 5 orders of magnitude lower ($\approx 10^{34}$ ergs s^{-1}) than the observed X-ray luminosity of SN 2006bp. Therefore, no significant contribution of the radioactive decay products to the total X-ray luminosity of SN 2006bp is expected. Recent simulations of the expected X-ray emission from Compton-scattered γ-rays of the radioactive decay products of the SN ejecta for SN 2005ke at early epochs (days) also shows the expected X-ray luminosity to be in the range 10^{33}–10^{34} ergs s^{-1} (Immler et al. 2006b), well below the observed X-ray luminosity of SN 2006bp.

This leaves either inverse Compton scattering or CSM interaction as the likely source of the detected X-ray emission. Since Type II-P SNe have a prolonged plateau period with high optical output associated with hydrogen recombination in the progenitor envelope, inverse Compton cooling of the relativistic electrons produced during the explosion by the photospheric photons might be important. Upscattering of the optical photons to energies in the X-ray range (depending on the Lorentz factor and the effective temperature of the photospheric emission) could produce a detectable X-ray flux during the first few days after outburst.

Chevalier et al. (2006) have shown that the X-ray luminosity of inverse Compton emission takes the form

$$\frac{dL_{\rm IC}}{dE} \approx \left(8.8\times10^{38}\right)\epsilon_r\gamma_{\rm min}E_{\rm keV}^{-1}\frac{\dot{M}_{-6}}{v_w}v_{s4} \times \frac{L_{\rm bol}(t)}{10^{42}\ {\rm ergs\ s^{-1}}}\left(\frac{t}{10\ {\rm days}}\right)^{-1}\ {\rm ergs\ s^{-1}\ keV^{-1}}, \quad (1)$$

where ϵ_r is the fraction of the postshock energy density that is in relativistic electrons, $\gamma_{\rm min}$ is the minimum Lorentz factor of the relativistic electrons, $\dot{M}_{-6}$ is the mass-loss rate (in units of $10^{-6}\,M_\odot$ yr^{-1}), v_w is the wind velocity (in units of km s^{-1}), v_{s4} is the SN shock velocity (in units of 10,000 km s^{-1}), and $L_{\rm bol}(t)$ is the bolometric luminosity at time t after the explosion. Assuming a mass-loss rate of $\dot{M} = (2\times10^{-6}\ M_\odot\ {\rm yr}^{-1})(v_w/10\ {\rm km\ s^{-1}})$ (see below), a shock velocity of 15,000 km s^{-1}, and a bolometric luminosity of $L_{\rm bol} = 10^{42}$ ergs s^{-1}, we estimate a monochromatic X-ray luminosity from inverse Compton scattering at 1 keV (near the peak of the *Swift* XRT and *XMM-Newton* EPIC response) of $L_{\rm X} \approx \epsilon_r\gamma_{\rm min}(4\times10^{39})$ ergs s^{-1}. The bolometric luminosity is justified by the modeling of SN II-P light curves (e.g., Chieffi et al. 2003).

Since the value for ϵ_r is expected to be in the range $\approx$0.01–0.1, a Lorentz factor of $\gamma_{\rm min} \approx 10$–100 is needed to satisfy the condition that all of the observed X-rays are due to inverse Compton scattering. As the most plausible value for the Lorentz factor for the shock velocities of SNe II-P is $\approx$1 (Chevalier et al. 2006), inverse Compton scattering is unlikely to account for the observed X-ray emission of SN 2006bp, although it cannot be ruled out entirely.

Alternatively, the X-ray emission might be caused by the interaction of the shock with the CSM, deposited by the progenitor's stellar wind. Of all 26 SNe detected in X-rays over the past three decades, the importance of inverse Compton scattering has only been discussed for two Type Ic SNe, SN 1998bw (Pian et al. 2000) and SN 2002ap (Bjornsson & Fransson 2004), while the remaining X-ray SNe have been discussed in the context of thermal emission (apart from the early emission of SN 1987A; see Park et al. [2006] and references therein).

If we assume a constant mass-loss rate $\dot{M}$ and wind velocity v_w from the progenitor's companion, the thermal X-ray luminosity of the forward shock region is $L_{\rm X} = [1/(\pi m^2)]\Lambda(T)(\dot{M}/v_w)^2(v_s t)^{-1}$ (Immler et al. 2006b), where m is the mean mass per particle (2.1×10^{-24} g for a H+He plasma), $\Lambda(T)$ is the cooling function of the heated plasma at temperature $T = 1.36\times10^9\left[(n-3)^2/(n-2)^2\right](v_s/10^4\ {\rm km\ s^{-1}})^2$ K (Chevalier & Fransson 2003), n is the ejecta density parameter (in the range 7–12), and v_s is the shock velocity. If we adopt an effective cooling function of $\Lambda_{\rm ff} = 2.4\times10^{-27}g_{\rm ff}T_e^{0.5}$ ergs cm^3 s^{-1} (Chevalier & Fransson 2003) for an optically thin thermal plasma with a temperature of T for the forward shock, where $g_{\rm ff}$ is the free-free Gaunt factor and $v_s = 15,000$ km s^{-1}, a mass-loss rate of $\dot{M} \approx (1\times10^{-5}\ M_\odot\ {\rm yr}^{-1})(v_w/10\ {\rm km\ s^{-1}})$ with an uncertainty of a factor of 2–3 is obtained. Assuming different plasma temperatures in the range 10^7–10^9 K would lead to changes in the emission measure by a factor of 3. The X-ray luminosity from shock-heated plasma behind the reverse shock is assumed to be small compared to that of the forward shock, since the expanding shell is still optically thick at such an early epoch. Since only high-quality X-ray spectra could give a conclusive answer to the contribution of the reverse shock to the total X-ray luminosity, our inferred mass-loss rate represents an upper limit. In the case in which the absorption is small and the bulk of the thermal emission originates in the reverse shock, the value of $\dot{M}$ is reduced by a factor of up to 10, assuming an ejecta density parameter of $n = 10$ (with a range between 7 and 12; see eq. [33] in Chevalier 1982).

While other core-collapse SN (Type Ib/c and II) progenitors can produce mass-loss rates as high as 10^{-5}–$10^{-3}\,M_\odot$ yr^{-1} due to the high masses and strong stellar winds of the progenitor stars, the mass-loss rate of the SN 2006bp progenitor is similar to those of other Type II-P SNe: a recent study of the thermal X-ray and radio synchrotron emission of a sample of Type II-P SNe (SN 1999em, SN 1999gi, SN 2002hh, SN 2003gd, SN 2004dj, and SN 2004et) gave mass-loss rate estimates of a few times $10^{-6}\,M_\odot$ yr^{-1} (Chevalier et al. 2006), characteristic of red supergiant progenitors, assuming stellar wind velocities for red supergiants of 10–15 km s^{-1}. Comparison shows that the SN 2006bp progenitor had a mass-loss rate similar to the lowest in this sample (SN 1999gi and SN 2004dj) and an mass of $\approx$12–15 $M_\odot$ prior to the explosion (see Fig. 1 in Chevalier et al. 2006) in the case in which the X-ray emission was dominated by the reverse shock.

CSM interaction gives an expected t^{-1} decline of the X-ray flux, consistent with the observed rate of decline (t^{-n}, with index $n = 1.2 \pm 0.6$). Inverse Compton scattering, on the other hand, only gives a t^{-1} decline when $L_{\rm bol}(t)$ is constant over time (as in the UVOT *V*-band light curve). However, at early times the blue/UV emission, which shows a fast rate of decline, contributes significantly to the bolometric luminosity, which leads to a faster X-ray rate of decline for inverse Compton scattering. Due to the large errors associated with the X-ray rate of decline, inverse Compton scattering cannot be entirely ruled out, but it is a less likely scenario for the production of the observed X-rays.

The distinguishing characteristic of the two emission processes is their spectrum (power law vs. thermal plasma). In the absence of high-quality spectra for the *Swift* XRT and *XMM-Newton* EPIC data, such a distinction cannot be made, since the *XMM-Newton* EPIC data are equally well fitted (using Cash statistics; Cash 1979) by a power law (best-fit photon index $\Gamma = 1.6^{+1.2}_{-0.7}$; $\chi^2 = 42.6$, dof = 52), a thermal plasma spectrum

(best-fit temperature $kT = 1.7$–27 keV, consistent with our spectral assumptions to infer fluxes; $\chi^2 = 42.3$, dof $= 52$), and a thermal bremsstrahlung spectrum (best-fit temperature $kT = 1.0$–179 keV; $\chi^2 = 41.4$, dof $= 52$).

5. SUMMARY

Starting at an age of $\approx$1 day after the outburst, our *Swift* observations of SN 2006bp represent the earliest X-ray observation and detection of a SN to date, apart from two explosions that were accompanied by a γ-ray signal (as in the case of SN 1998bw/GRB 980425, which *BeppoSAX* started observing 12 hr after the outburst [Pian et al. 2000], and SN 2006aj/GRB 060218, for which prompt X-ray emission was detected [Campana et al. 2006]). SN 2006bp faded below the *Swift* XRT sensitivity limit within less than 2 weeks, and a more sensitive *XMM-Newton* observation recovered the SN 3 weeks after its explosion. Broadband SEDs and, in particular, UV spectra of SNe show the importance of and give insights into line blanketing during the early phase in the evolution.

Currently *Swift* is the only telescope capable of revealing the fast changes in the UV flux from SN explosions, offering sensitive constraints on the ionization state in the continuum and line formation region of the ejecta, the sources of metal line blanketing. By extending the spectral coverage, this provides stronger constraints on the reddening, as well as complementary information to what can be deduced from optical observations alone. While there is ample evidence for diversity in Type II SN optical spectra, *Swift* observations can be used to address the existence of a corresponding diversity in the UV range.

The detection of SN 2006bp in X-rays at such an early epoch, as well as the detection of its fast optical/UV spectral evolution, was made possible by the quick response of the *Swift* satellite and underlines the need for rapid observations of SNe in the UV and in X-rays. It should be pointed out that the response time of all previous X-ray observations of SNe (with missions such as *Einstein*, *ASCA*, *ROSAT*, *Chandra*, and *XMM-Newton*) were in the range between >4 days (SN 2002ap) and a few weeks. The bulk of all X-ray observations took place weeks to months after the explosions. Therefore, if SN 2006bp is more typical for a larger sample of core-collapse SNe, then the early production of X-rays would have been missed in each of the previous cases. The response time of our ongoing *Swift* observing program to study the prompt emission of SNe across the optical, UV, and X-rays is currently only limited by the time lag between the explosion of a SN and its discovery at optical wavelengths and timely alert by the community.

We gratefully acknowledge support provided by STScI grant HST-GO-10182.75-A (P. A. M.), NASA Chandra Postdoctoral Fellowship grant PF4-50035 (D. P.), and NSF grant AST 03-07366 (R. A. C.). L. D. acknowledges support for this work from the Scientific Discovery through Advanced Computing (SciDAC) program of the DOE, grant DE-FC02-01ER41184, and from the NSF under grant AST 05-04947. K. W. W. thanks the Office of Naval Research for the 6.1 funding supporting this research. C. J. S. is a Cottrell Scholar of Research Corporation, and work on this project has been supported by the NASA Wisconsin Space Grant Consortium.

This work is sponsored at Pennsylvania State University by NASA contract NAS5-00136. We wish to thank N. Schartel and the *XMM-Newton* SOC for approving and scheduling a *XMM-Newton* DDT observation. The research has made use of the NASA/IPAC Extragalactic Database (NED), which is operated by the Jet Propulsion Laboratory, California Institute of Technology, under contract with the National Aeronautics and Space Administration.

REFERENCES

Baron, E., Hauschildt, P. H., & Branch, D. 1994, ApJ, 426, 334
Bjornsson, C.-I., & Fransson, C. 2004, ApJ, 605, 823
Blinnikov, S., & Bartunov, O. S. 1993, A&A, 273, 106
Blinnikov, S., Eastman, R. G., Bartunov, O. S., Popolitov, V. A., & Woosley, S. E. 1998, ApJ, 496, 454
Blinnikov, S., Lundqvist, P., Bartunov, O. S., Nomoto, K., & Iwamoto, K. 2000, ApJ, 532, 1132
Burrows, D. N., et al. 2005, Space Sci. Rev., 120, 165
Campana, S., et al. 2006, Nature, 442, 1008
Cash, W. 1979, ApJ, 228, 939
Chevalier, R. A. 1982, ApJ, 259, 302
Chevalier, R. A., & Fransson, C. 2003, in Supernovae and Gamma-Ray Bursters, ed. K. W. Weiler (Berlin: Springer), 171
Chevalier, R. A., Fransson, C., & Nymark, T. K. 2006, ApJ, 641, 1029
Chieffi, A., Domínguez, I., Höflich, P., Limongi, M., & Straniero, O. 2003, MNRAS, 345, 111
Dessart, L., & Hillier, D. J. 2005, A&A, 437, 667
———. 2006, A&A, 447, 691
Dickey, J. M., & Lockman, F. J. 1990, ARA&A, 28, 215
Eastman, R. G., & Kirshner, R. P. 1989, ApJ, 347, 771
Ensman, L., & Burrows, A. 1992, ApJ, 393, 742
Fransson, C., Grewing, M., Cassatella, A., Wamsteker, W., & Panagia, N. 1987, A&A, 177, L33
Fransson, C., Lundqvist, P., & Chevalier, R. A. 1996, ApJ, 461, 993
Fransson, C., et al. 2002, ApJ, 572, 350
Gehrels, N., et al. 2004, ApJ, 611, 1005
Heger, A., Fryer, C. L., Woosley, S. E., Langer, N., & Hartman, D. H. 2003, ApJ, 591, 288
Immler, S., Brown, P., & Milne, P. 2006a, ATel, 793, 1
Immler, S., et al. 2006b, ApJ, 648, L119
Jeffery, D. J., et al. 1994, ApJ, 421, L27
Kelley, M. T., Stockdale, C. J., Sramek, R. A., Weiler, K. W., Immler, S., Panagia, N., & van Dyk, S. D. 2006, Cent. Bur. Electron. Telegrams, 495, 1
Lentz, E. J., Baron, E., Branch, D., Hauschildt, P. H., & Nugent, P. E. 2000, ApJ, 530, 966
Li, L.-X. 2007, MNRAS, 375, 240
Lundqvist, P., & Fransson, C. 1988, A&A, 192, 221
Mazzali, P. A. 2000, A&A, 363, 705
Mazzali, P. A., & Chugai, N. N. 1995, A&A, 303, 118
Mazzali, P. A., & Lucy, L. B. 1993, A&A, 279, 447
McCray, R. 1993, ARA&A, 31, 175
Nakano, S. 2006, Cent. Bur. Electron. Telegrams, 470, 1
Park, S., et al. 2006, ApJ, 646, 1001
Pian, E., et al. 2000, ApJ, 536, 778
Pun, C. S. J., et al. 1995, ApJS, 99, 223
———. 2002, ApJ, 572, 906
Quimby, R., Brown, P., Caldwell, J., & Rostopchin, S. 2006, Cent. Bur. Electron. Telegrams, 471, 1
Roming, P. W. A., et al. 2005, Space Sci. Rev., 120, 95
Verheijen, M. A. W., & Sancisi, R. 2001, A&A, 370, 765
Weiler, K. W., Panagia, N., Montes, M. J., & Sramek, R. A. 2002, ARA&A, 40, 387